ChemCatChem

Supporting Information

Role of Copper Migration in Nanoscale Ageing of Supported CuO/Al_2O_3 in Redox Conditions: A Combined Multiscale X-ray and Electron Microscopy Study

Sharmin Sharna, Virgile Rouchon, Christèle Legens, Anne-Lise Taleb, Stefan Stanescu, Corinne Bouillet, Arnold Lambert,* Valerie Briois, David Chiche, Anne-Sophie Gay, and Ovidiu Ersen

SI.1: Beamline presentation, data acquisition and data treatment

The STXM analyses were carried out on the HERMES beamline of the SOLEIL synchrotron [1]. The HERMES beamline drives two microscopes, STXM and XPEEM (X-ray PhotoEmission Electron Microscopy). The beamline utilises a beam in the energy range of 70 eV to 1.6 keV and covers the K-edge of light elements (C, N, O..), L-edge of transition metals, and M,N-edges of rare earths. The beamline uses two undulators such as to cover the entire energy range from 70 to 1600 eV.
The STXM equipment is presented in Figure S1. The energy range of the HERMES beamline is particularly advantageous to probe both the copper and aluminium chemical coordination, thus providing a complete picture of the sample's local environment. In the current experiments, the sample was probed at the Cu $L_{2,3}$-edges and Al K-edge. A Fresnel zone plate (FZP) with the outermost lines of 35 nm was used, providing a theoretical beam spot size on the sample of about 43 nm.

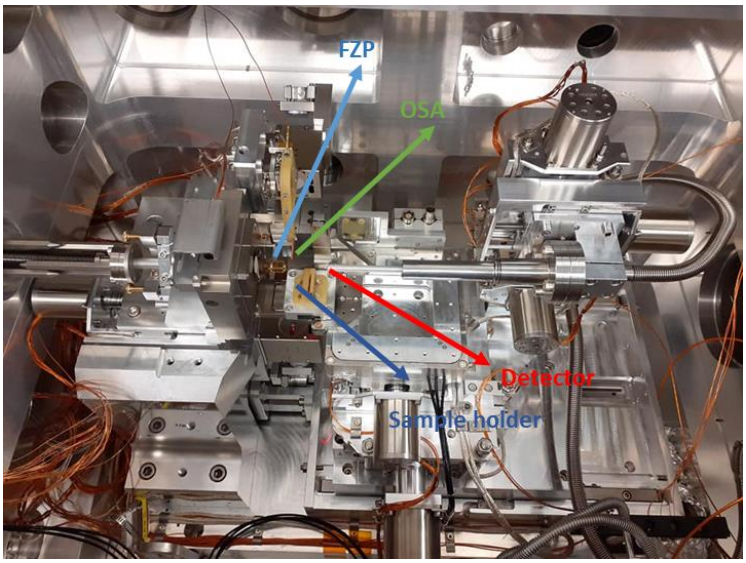

Figure S1: STXM picture at the HERMES beamline, showing FZP, Order Sorting Aperture (OSA), sample holder and detector.

Data acquisition and analysis
Three types of scans were performed: lines, mappings (high-resolution spatial images recorded at few specific energies) and energy stacks (full hyperspectral 3D datasets recorded across Cu $L_{2,3}$ and Al K absorption edges). In the line scan mode we define a line composed of several spatial points that are scanned over a large photon energy range. Typically, this mode can be used if we assume homogenous material in the sample scanning both through the sample and a free, I_0 region. This results in a faster recording scheme with good statistics, since the final spectra is obtained by summing over all points corresponding to the measured material (particle)Therefore the line scan mode was used exclusively for the reference materials.
For the samples, two modes of acquisition called "mapping" scan with a higher spatial resolution (10 x 10µm, 0.030 µm step-size) and "energy stack" (4 x 4 µm, 0.08 µm step-size) were used.
In mapping mode, we acquire images at few selected energies extracted from overall energy scans. An energy stack consists in a series of images acquired over a large energy range and

allows to obtain a 3D dataset in x, y, and energy dimensions. Thus, each pixel contains a full spectrum.
In practice, we first recorded energy stacks, isolate particular spectral features and then mapped larger areas of the sample at these specific energies. This way we could distinguish both particular phases developing in our materials and to locate them precisely.
The scan parameters for the different modes are provided in **Table S.*1***. The energy step Cu L-edge scan was adjusted to be faster at the beginning and end of the energy range, 0.5 eV for 920-929 eV and 960 – 970 eV. Between 929 and 960 eV which is the edge range, a shorter step-size was used: 0.15 eV from 929 – 940 eV, 0.35 eV for 940 – 950 eV and 0.15 eV for 950-960 eV. For the Al K-edge, an energy step of 0.18 eV was used for the whole 1570 – 1600 eV energy range. A dwell time of 3 ms was gave enough statistics to describe both edges.

Table S.1: Scan parameters used for the data acquisition in different scan modes.

Scan	Energy (eV)	Dimension (µm)	Step size (µm)	Dwell time (ms)	Total duration
Line	Cu: 920 – 970	5	0.1	1	14 min 30 s
	Al: 1570 – 1600	5	0.1	1	14 min
Map	Cu: 920, 933, 934, 936.6, 940.4 and 950	10 x 10	0.03	3	1 h 44 min
	Al: 1570, 1578, 1581, 1584 and 1591	10 x 10	0.03	3	1 h 27 min
Stack	Cu: 920 – 970	4 x 4	0.08	3	1 h 50 min
	Al: 1570 – 1600	4 x 4	0.08	3	1 h 30 min

Additionally, I_0 was measured during the acquisition of the line and stack. The I_0 area used for the I_0 acquisition was chosen without the presence of the feature of interest, typically, in an area with polymer resin of the sectioned samples.
Data treatment was carried out using AXis2000 software developed by Prof. Adam Hitchcock from McMaster University in Canada [2].
The line scan data was treated by taking the I_0 into account, to acquire the reference spectra.
Since the mapping was carried out at specific energies, typically at the absorption energy of the known phases, false color coded images can be obtained assigning a color to each of the spectral component recorded.
As demonstrated in Figure S.*2* the first step of stack data treatment involves drift correction by aligning the series of images, using a built-in function called “Jacobsen stack analyses” based on the Fourier cross-correlation method. Using the I_0 measurement as a reference point for the X-ray photon transmission, the transmission images are converted into optical density (OD) images. A typical stack contains about 2000-3000 spectra and usually less than 6 statistically significant species. In order to extract the principal components in the area of interest, spectra can be extracted as single component from an OD stack and used as a reference to generate the spatial distribution of the respective chemical components either using the Singular Value decomposition (SVD) or stack fit method. Both SVD and stack fit functions use the SVD algorithm.
Sets of component maps can be combined into colour composite maps displaying the relative spatial distribution of the individual components. A quantitative analysis could be achieved by reducing the individual spectral components to OD1 (i.e. OD per 1 nm), such as to represent color-coded images in thickness units per color.

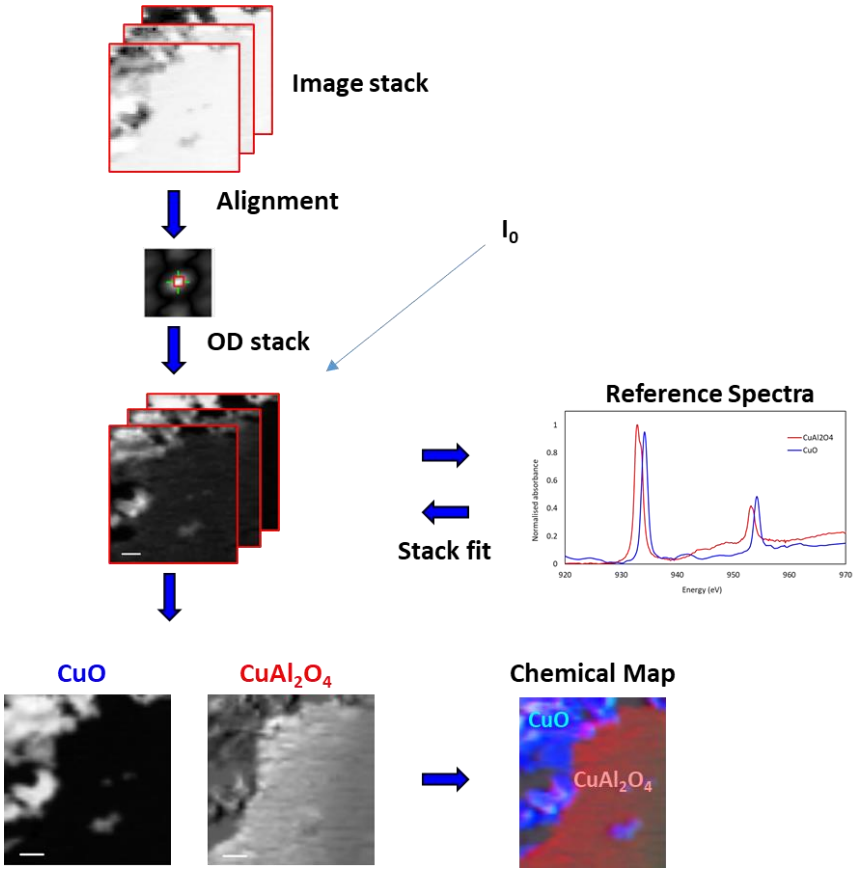

Figure S.2: Outline of processing of a STXM stack process of CuO/Al_2O_3 sample. The image stack is measured in transmission mode by STXM at Cu L-edge (920 – 960 eV), drift correction using cross-correlation method, conversion to OD stack considering I_0 background, generated component spectra from reference, stack fit using reference spectra, composite chemical map (blue is CuO, red is $CuAl_2O_4$).

Sample preparation

Soft X-rays are known to interact strongly with matter implying that the sample thickness is an important consideration. Strong absorption can modify the spectral shape and the apparent optical density due to non-linear absorption [3]. Therefore, the sample should be thin enough for the transmission of the beam and to avoid absorption saturation. The concentration of the sample, the choice of the edge and the edge energy determine the adequate thickness of the sample. For our samples the thickness was calculated to be less ~100 nm, using the Centre for X-ray Optics (CXRO) website [4].

Hence, ultramicrotomy sectioning was performed on capsules of impregnated bead powders in TEM resin to a thickness of 100 nm and placed on Au (200 mesh, carbon coated) TEM grids. The region of interest was identified using SEM in STEM-HAADF imaging mode (~2 nm resolution @ 40kV) in SEM. In addition to the thickness, the sectioning of the sample preserved the structure of the support grain and the spatial information of the different copper-alumina phases.

Oxidation-sensitive samples such as reference metallic Cu, Cu_2O, and the cycled oxygen carrier in reduced state, were prepared inside a glovebox. The samples were crushed and deposited on a 50 nm thickness SiN_x membrane and sealed with another SiN_x membrane.

The other reference samples were simply crushed and deposited on an Au grid and glued to the sample holder with silver glue. An example of the sample holder is shown in Figure S.3.

Figure S.3: Sample holder with glued TEM grid.

Al K-edge features and assignments

Table S.2 : Al K-edge features and assignments of the energies

Compound	Energy (eV)	Assignment
α-Al_2O_3	1578.0	1s → 2s-σ* (a_{1g})
	1580.8	1s → 3p-σ/π* (t_{1u})
	1584.9	1s → 3d-σ* (t_{2g})
γ- Al_2O_3	1579.0	1s → 3p-σ/π* (t_2)
	1581.0	1s → 3p-σ/π* (t_{1u})
	1584.0	1s → 3d-σ* (t_{2g})
$CuAl_2O_4$	1578.9	1s → 3p-σ/π* (t_2)
	1580.8	1s → 3p-σ/π* (t_{1u})
	1584.5	1s → 3d-σ* (t_{2g})

SI.2: X-ray Absorption Spectroscopy – at Cu K-edge

Reference Samples

For the references, mainly CuO, stoichiometric copper aluminate and non-stoichiometric copper aluminate phases are chosen since the samples were in oxidized state during the post-mortem characterisation. The energy scale of the data was calibrated using the maximum of the first derivative of the Cu foil at 8979 eV.

For the CuO reference, commercial powder from Sigma Aldrich is used.

The $CuAl_2O_4$ sample was prepared by mechanically mixing and grinding 1:1 molar ratio of CuO powder (from Sigma Aldrich) and Al_2O_3. The mixture was calcined at 600 °C for 12 hours, to avoid the formation of alpha Al_2O_3. The process of grinding and calcination was repeated one more time at 600 °C and finally at 900 °C for 12 hours.

For the non-stoichiometric copper aluminate reference, the fresh CuO/Al_2O_3-900 sample is considered. As stated in the article, the sample is very heterogenous with a range of copper percentage in the copper aluminate phase which affects the spectral feature of the aluminate phase as s function of the local copper concentration. Since XAS provides a global feature of the sample and knowing that the sample do not contain any CuO phase (confirmed from XRD and linear combination fitting), the CuO/Al_2O_3-900 was chosen to represent non-stoichiometric copper aluminate with a overall copper concentration of 10.4 wt%.Figure S.4 display the spectra of the three phases.

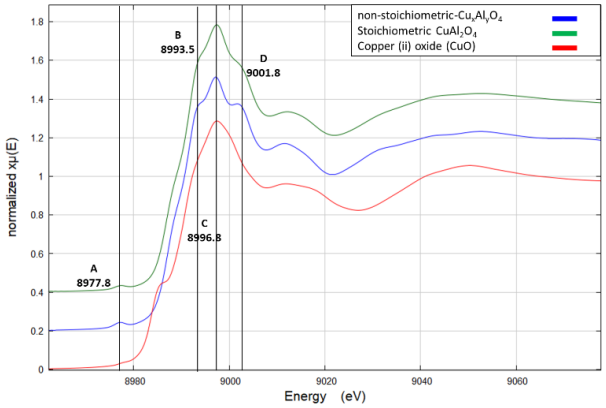

Figure S.4: Cu K edge XAS spectra of the reference phases of copper – copper (ii) oxide (red), stoichiometric copper aluminate ($CuAl_2O_4$) and non-stoichiometric copper aluminate ($Cu_xAl_yO_4$).

The CuO K-edge spectrum is characterized by three peaks representing the pre-edge (A at 8978 eV) for the 1s → 3d transition, B (8986 eV) is due to the 1s→ 4 p shakedown and C (8994 eV) is due to 1s → 4p continuum transition [5]. The pre-edge peak is specific to Cu(II) species due to the presence of $3d^9$ configuration. For all the two aluminate spectra, the 4 distinct peaks are noted. Peak A at about 8978 eV is a pre-edge peak resulting from 1s → 3d transition, similar to CuO [6]. Peaks B to D result from the different Cu atoms environments (tetrahedral and octahedral sites) present in the copper aluminate phase [7].

As noted from the spectra the two shoulder peaks on both sides (B and D) of the aluminate phase tend to become less prominent with decrease in the amount of copper. This characteristics change with the structural copper content is demonstrated by Shimizu et al [8].

SI.2.1. Fresh samples

(a) Fresh CuO/Al_2O_3-700

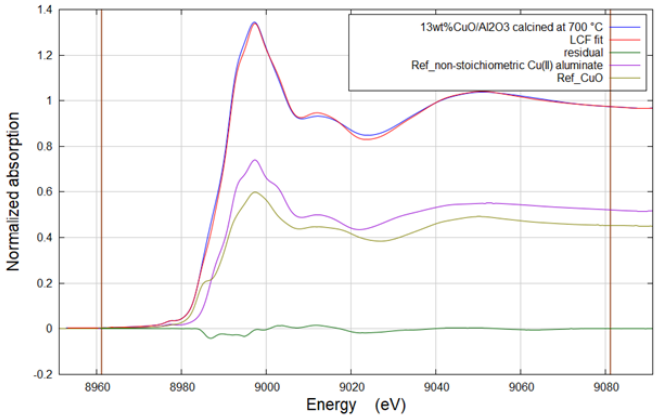

(b) Fresh CuO/Al_2O_3-800

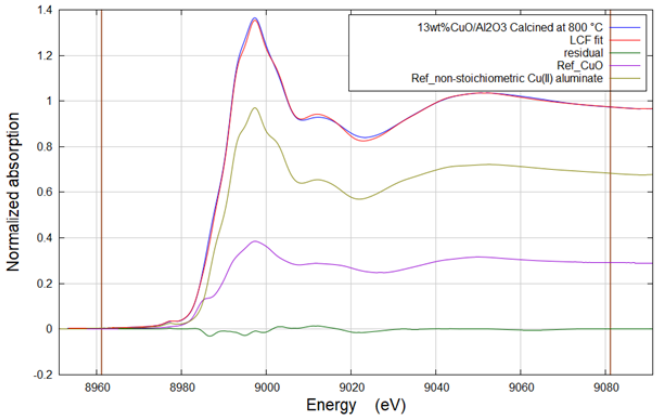

(c) Fresh CuO/Al_2O_3-900

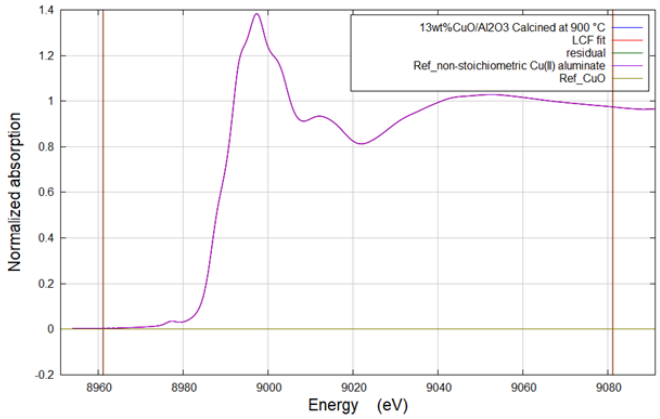

Figure S.3: Linear combination fitting of the Cu K edge XAS spectra of fresh CuO/Al_2O_3 samples calcined at 700, 800 and 900 °C.

SI.2.2. CuO/Al_2O_3-900 cycled samples

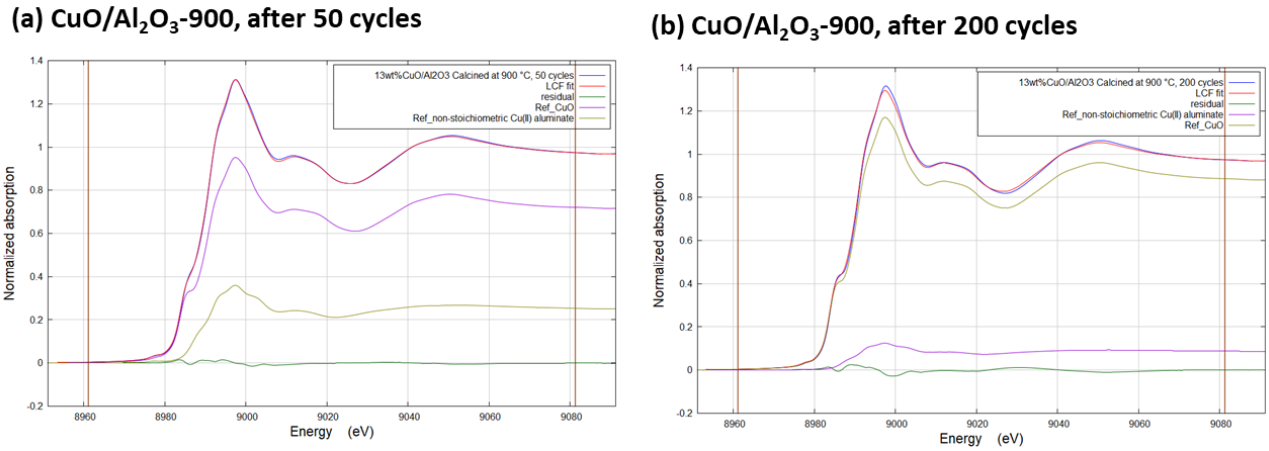

Figure S.5: Linear combination fitting of the Cu K edge XAS spectra of CuO/Al_2O_3-900, after 50 and 200 cycles.

SI.2.3. CuO/Al_2O_3-800 cycled samples

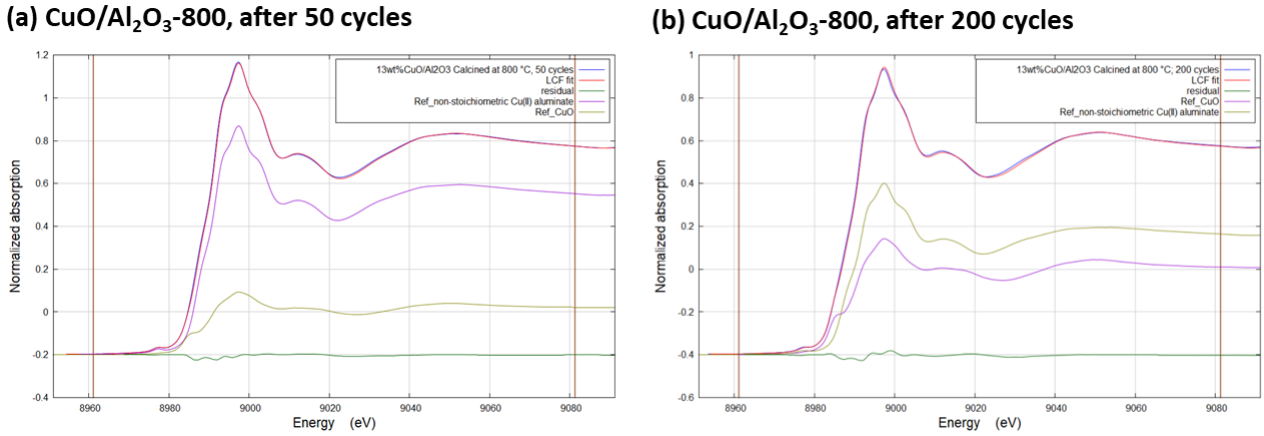

Figure S.6 Linear combination fitting of the Cu K edge XAS spectra of CuO/Al_2O_3-800, after 50 and 200 cycles.

SI.2.4. CuO/Al_2O_3-700 cycled sample

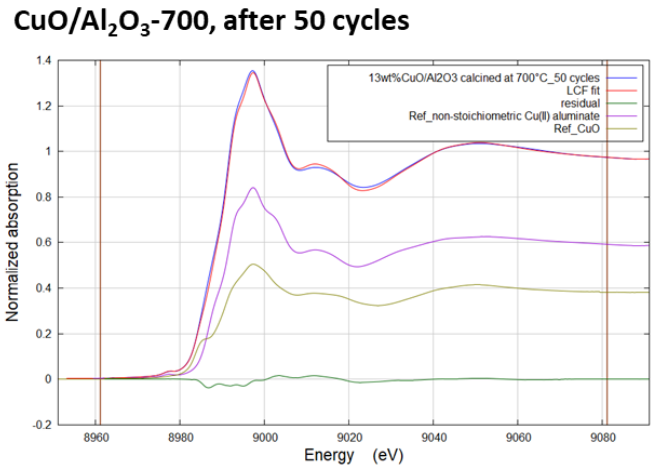

Figure S.7 : Linear combination fitting of the Cu K edge XAS spectra of CuO/Al_2O_3-700, after 50 cycles.

SI.3. X-ray diffraction data

SI.3.1. CuO/Al_2O_3-900 cycled samples

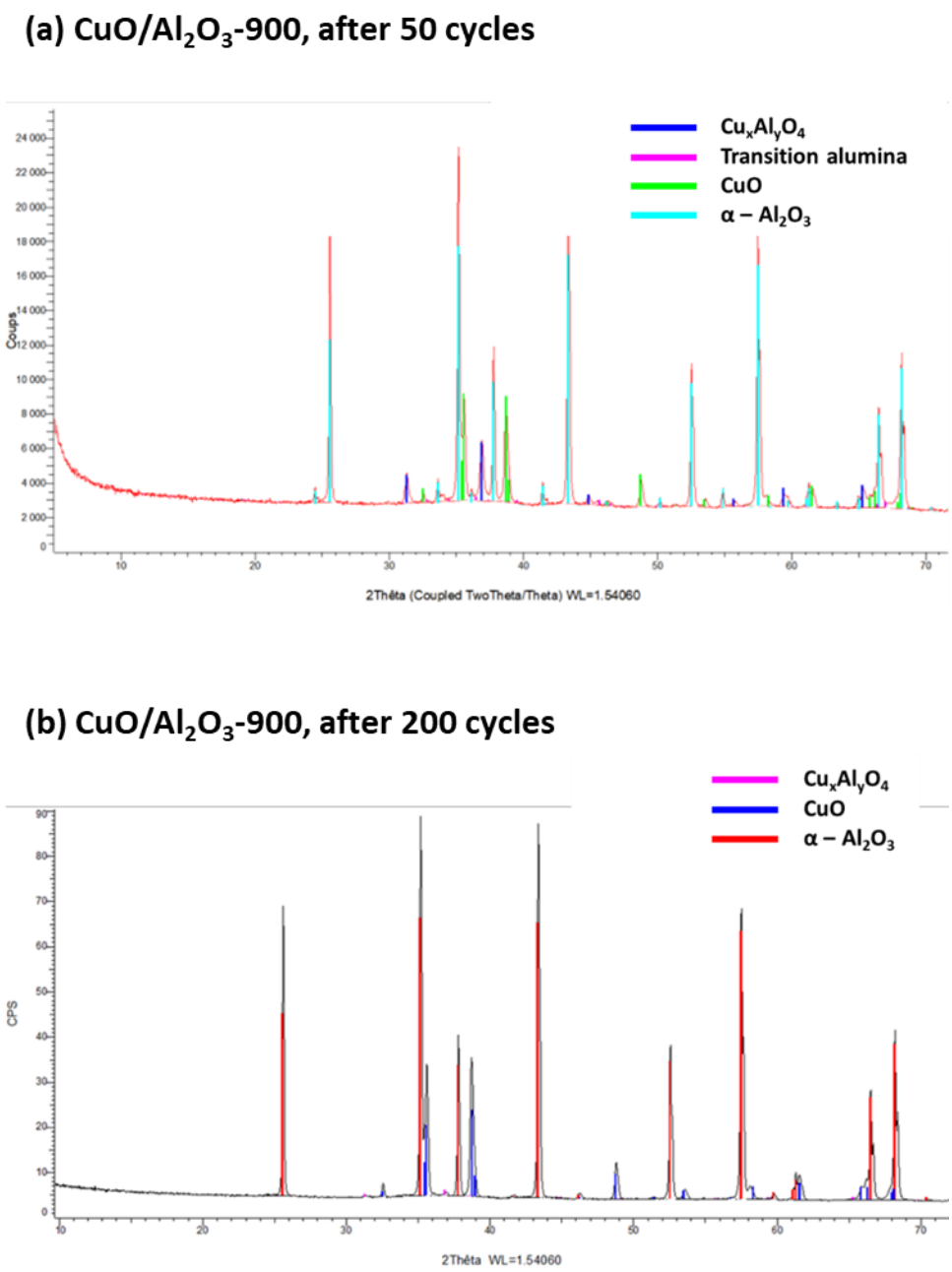

Figure S.8 : XRD of the CuO/Al_2O_3 – 900 °C sample, after 200 cycles.

SI.3.2. CuO/Al_2O_3-800 cycled samples

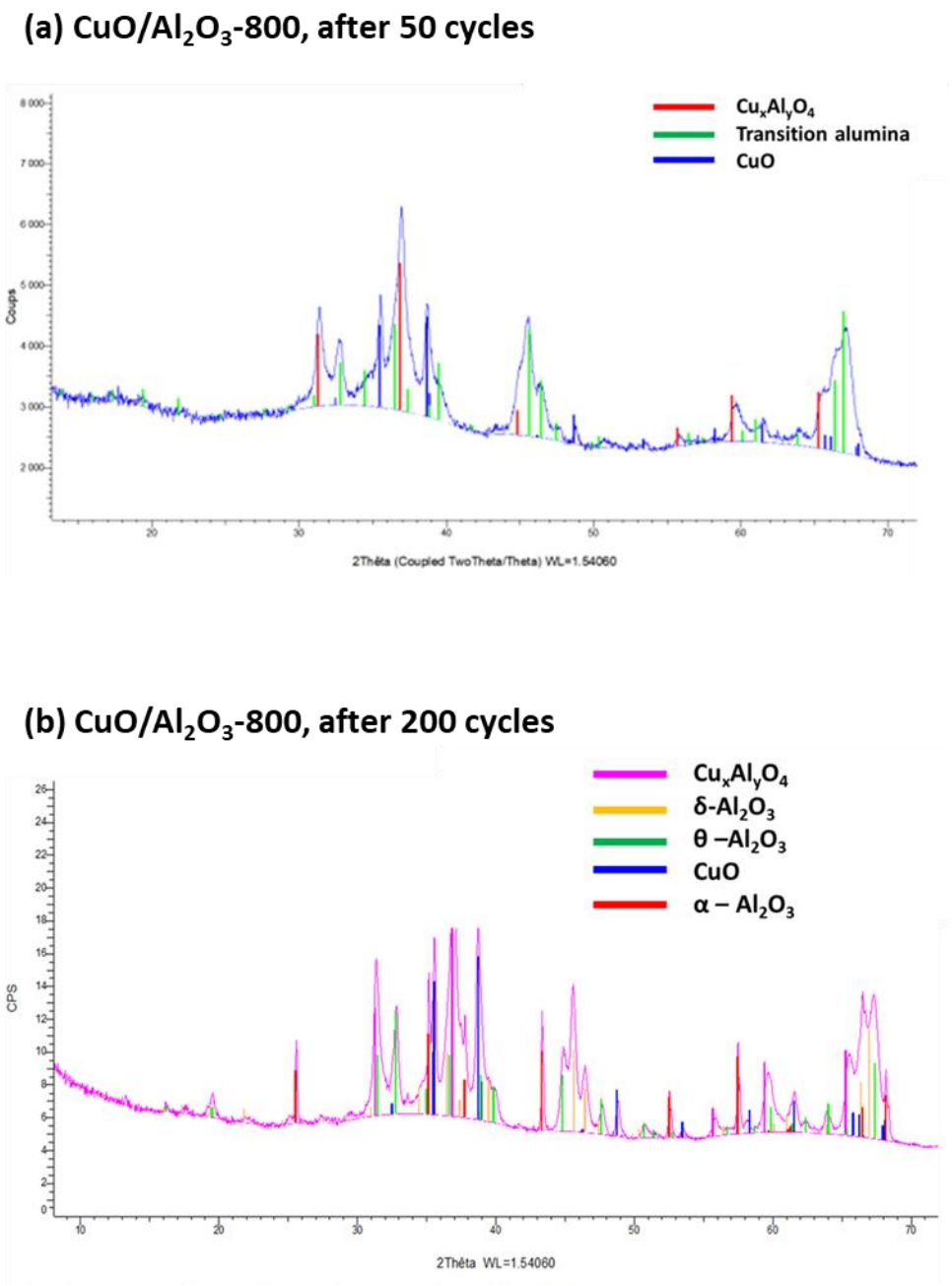

Figure S.9: XRD of CuO/Al_2O_3-800 °C sample, after 200 cycles.

SI.3.3. CuO/Al_2O_3-700 cycled samples

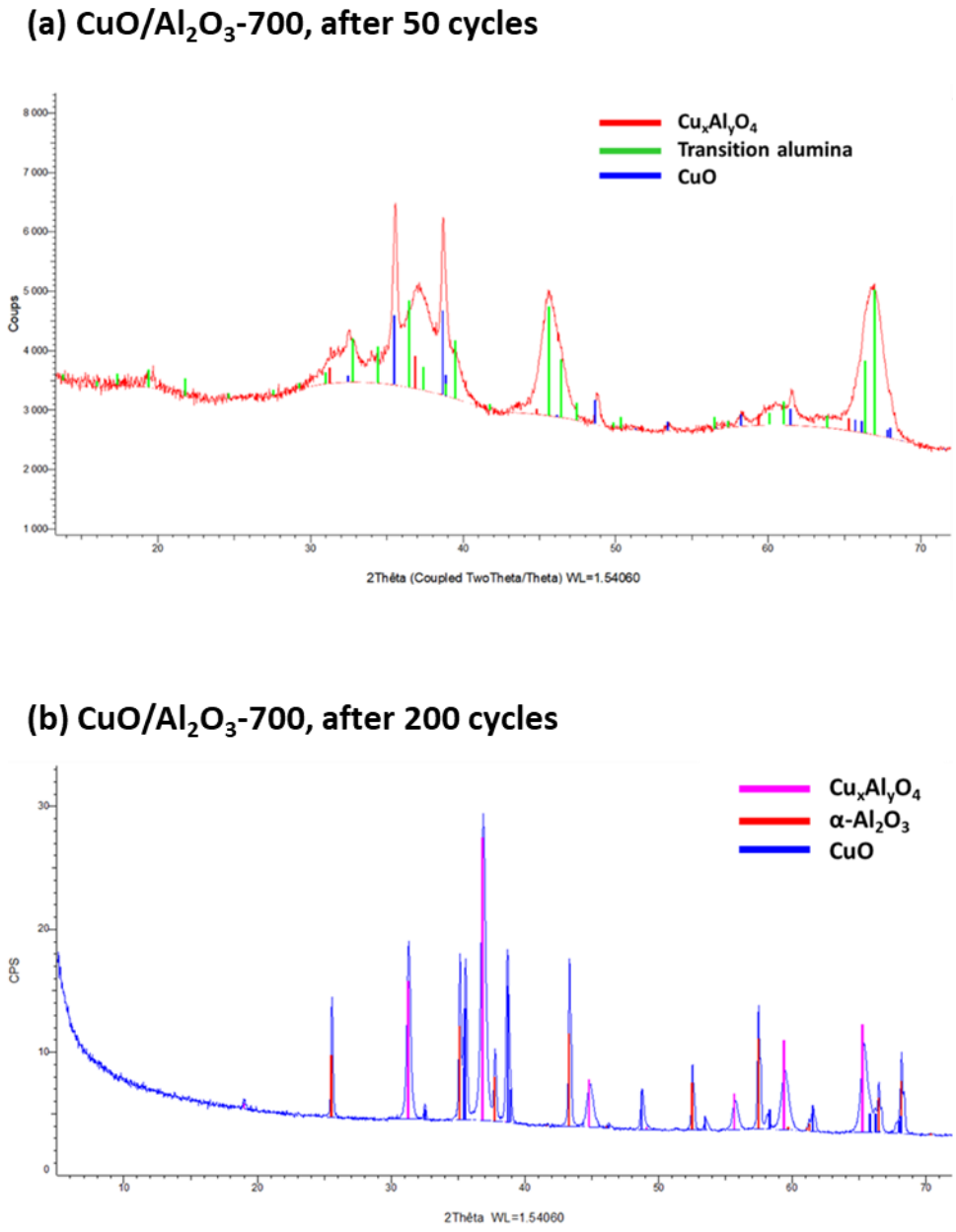

Figure S.10: XRD of CuO/Al_2O_3-700 °C sample after 200 cycles.

SI.4: In-situ X-ray diffraction

SI.4.1. Calcination of fresh CuO/Al_2O_3-800 sample from 800 °C to 900 °C

To observe the formation of the copper aluminate phase at the expense of the CuO as well as to understand the α-Al_2O_3 formation, the CuO/Al_2O_3 – 800 °C sample has been subjected to calcination from room temperature to 900°C under air and the evolution was followed by in situ XRD to identify the possible phase transitions in the temperature range of 800 – 900 °C.
The sample was first heated from room temperature to 780 °C at a rate of 5 °C/min and, subsequently, at a rate of 1 °C from 780 °C to 800 °C. As the temperature reached 800 °C, heating was carried out in stages of 10 minutes of heating at every 10 °C, at 1 °C/min rate. X-ray diffraction acquisition was conducted from 25 to 70 ° in 2θ with a step size of 0.083 °/s. With this setup and experimental conditions, 1 diffractogram was acquired every 10 minutes.
Figure S.*11* displays the diffractograms obtained at every 10 °C, from 800 to 900 °C during the annealing of the oxygen carrier. As mentioned already in the article, the sample is composed of CuO and a mixture of sub-stoichiometric $Cu_xAl_yO_4$ and transition alumina. Above 830 °C, the peaks corresponding to the CuO phase start to decrease, disappearing completely as the temperature reached 860 °C. The disappearance of the CuO phase is linked to the diffusion of copper in the alumina matrix to form copper aluminate. The initial sample is composed of poorly crystalline Cu-aluminate and after the calcination at 900 °C, the peak positions of the (400) and (440) Miller indices of alumina (46 ° and 66 ° in 2θ, resp.) moved to lower 2θ, gradually reaching towards the peaks positions of the aluminate phase. The displacement of the peak position to lower 2θ is linked to the increase in the d-spacing and the lattice parameter due to the addition of the Cu^{2+} in the alumina spinel.

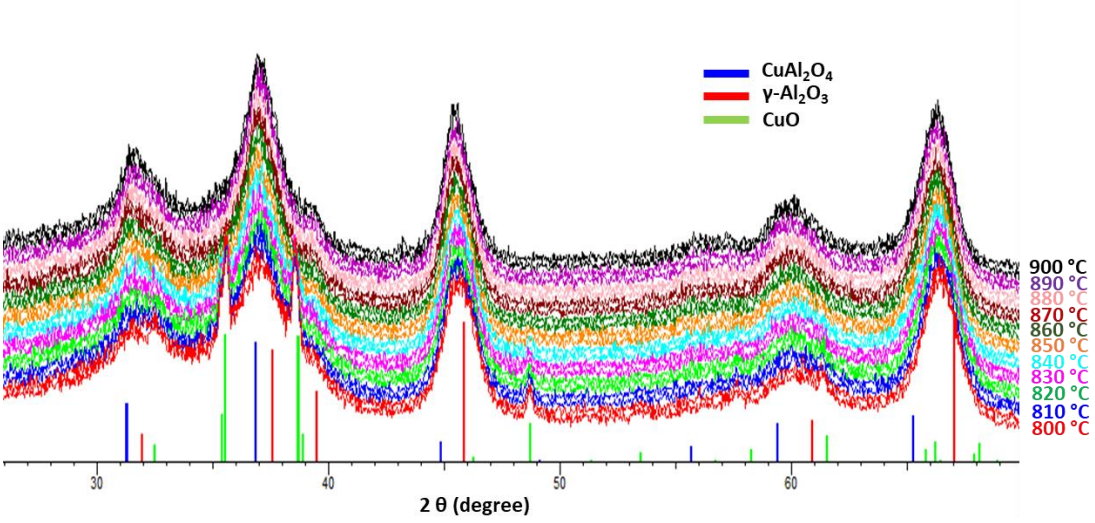

Figure S.11 : In situ XRD during the thermal annealing of the CuO/Al_2O_3-800 °C sample from 800 °C to 900 °C, under air.

The presence of α-Al_2O_3 phase was not observed in these conditions. To detect the α-Al_2O_3 phase by XRD, the sample should probably have been heated at 900°C for a longer duration.

SI.4.2. Effect of cycling temperature on the fresh material calcined at 900°C

The effect of the cycling at a temperature of 700 °C on the fresh oxygen carrier calcined at 900 °C, was monitored using in situ XRD. As mentioned previously, the sample is initially mainly composed of $Cu_xAl_yO_4$, transition alumina and α-Al_2O_3.
The evolution of diffractograms as a function reaction gas is presented in Figure S.*12*. At the first reduction step the initial $Cu_xAl_yO_4$ phase directly reduces to metallic copper. No

intermediate of copper oxide phase is observed. The peak of the $Cu_xAl_yO_4$ is broadened with a gradual loss of intensity during the first few minutes.
During the reoxidation, the copper is first oxidised to Cu_2O and then the Cu_2O slowly disappears to reform the $Cu_xAl_yO_4$ phase. The reformation of $Cu_xAl_yO_4$ occurs either directly from Cu_2O or via CuO phase. The peak intensity and shape is relatively sharper than the Cu-deficient aluminate, after the reduction step. The CuO intensity is weak in the 1st redox cycle.
Similar reactions occur during the 2nd and 3rd redox cycles. With every reduction-oxidation reaction, the CuO peaks' intensity increase, while the $Cu_xAl_yO_4$ peaks' intensity fades, and the peaks' shape broaden. For the $Cu_xAl_yO_4$ phase, the peak positions slowly shifted to higher 2θ values (by 0.2° 2θ) or lower d-spacing values indicating a decrease in the lattice parameter values. With the conversion of copper from the aluminate phase to CuO, the concentration of copper in $Cu_xAl_yO_4$ phase is reduced. Additionally, due to the relatively low temperature of the reaction, the diffusion of copper might be hindered. The peak broadening could either stem from the low copper concentration and/or presence of structural defects. No change in the α-Al_2O_3 phase is noted.
Over these three cycles at 700°C, CuO accumulates, hence the Cu deficient spinel peaks move towards the position of γ-Al_2O_3. Since no alpha alumina is formed, the $Cu_xAl_YO_4$ slowly moves back to Al_2O_3.

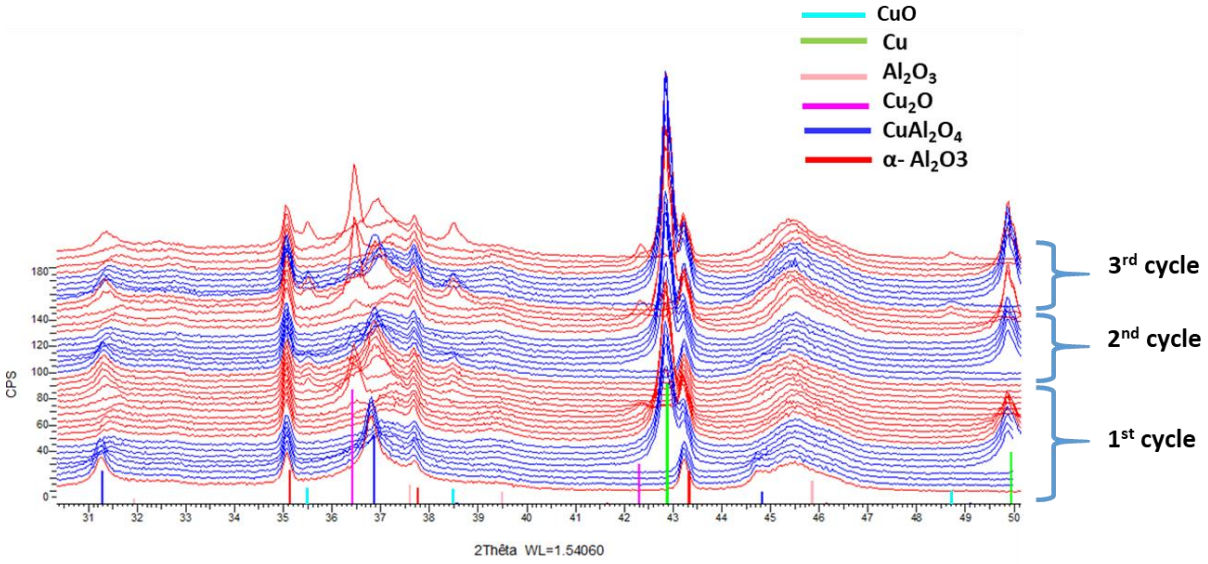

Figure S.12: in situ XRD of the redox cycling of CuO/Al_2O_3-900 °C sample at 700 °C. The blue and red spectra represent the sample during oxidation and reduction, respectively.

The redox induced phase transition is determined by the temperature of redox cycling. Even if the initial sample is composed of $Cu_xAl_yO_4$ phase, the reformation of the copper aluminate from reduced copper is a diffusion-controlled reaction which would either require high reaction temperature or longer duration of heating. Bolt et al. specified that the grain boundary diffusion of copper in polycrystalline γ-Al_2O_3 is faster than the bulk diffusion [9]. Thus, the accumulation of copper oxide is more likely at 700 °C.

SI.5: SEM, STEM and EDS

SI.5.1. Fresh CuO/Al_2O_3 800

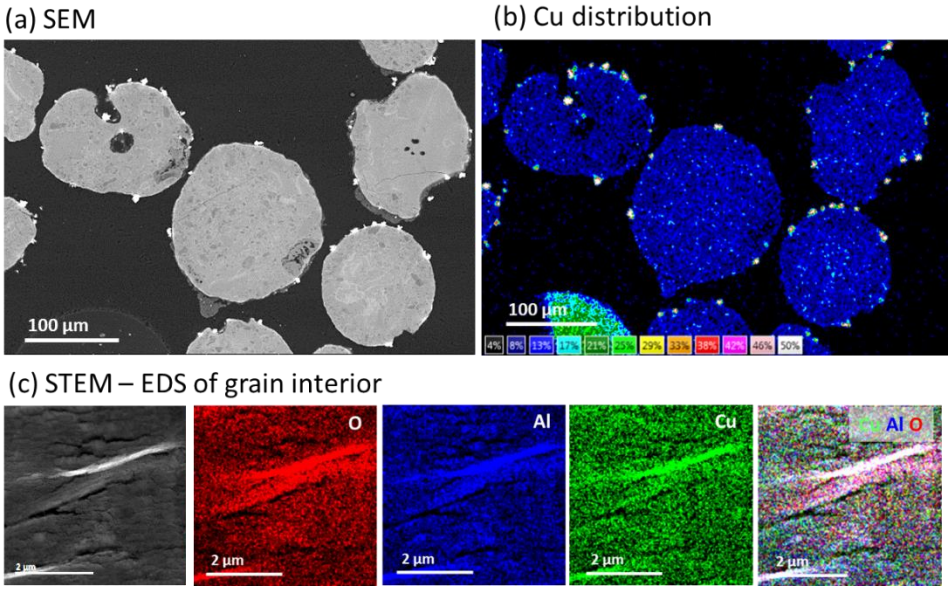

Figure S.13: a) SEM, b) distribution of copper in the grain and c) STEM-EDS of the interior of the grain of fresh CuO/Al_2O_3-800 sample.

SI.5.2. Fresh 900

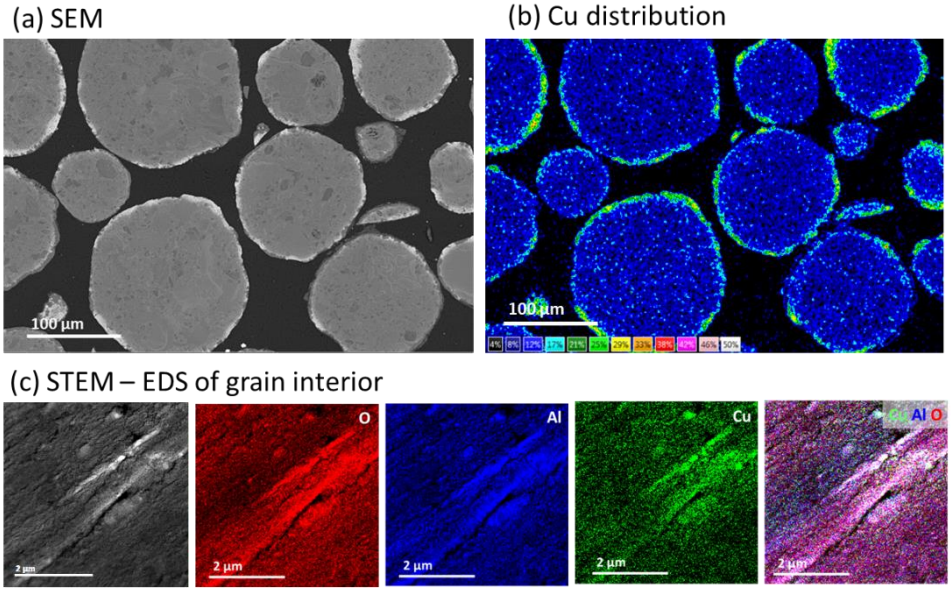

Figure S.14 : a) SEM, b) distribution of copper in the grain and c) STEM-EDS of the interior of the grain of fresh CuO/Al_2O_3-900 sample.

SI.5.3. 800 after 50 cycles

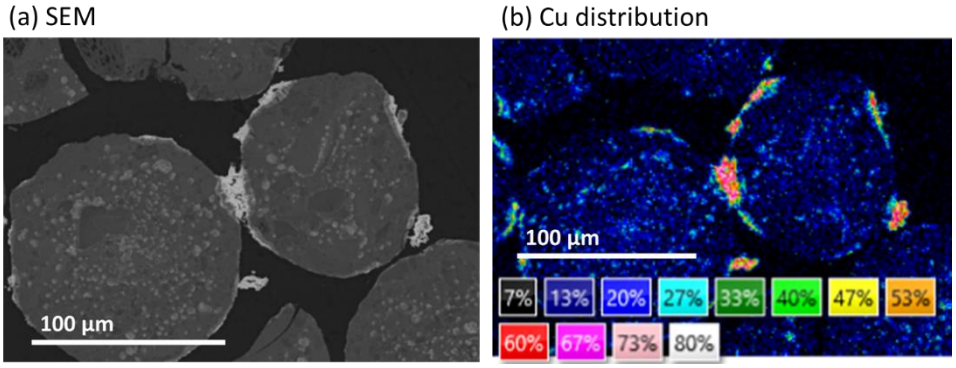

Figure S.15: a) SEM image and b) EDS Cu-concentration map of the sample cycled at 800 °C, after 50 cycles.

SI.5.4. 800 after 200 cycles

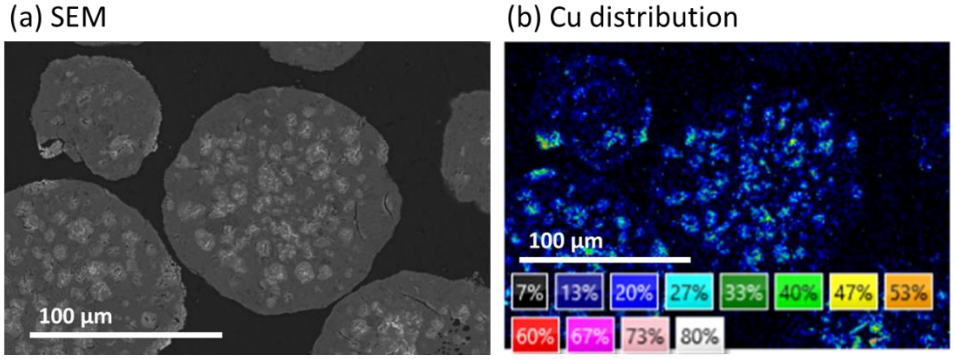

Figure S.16: a) SEM image and b) EDS Cu-concentration map of the sample cycled at 800 °C, after 200 cycles.

SI.5.5. 700 – 50 cycles

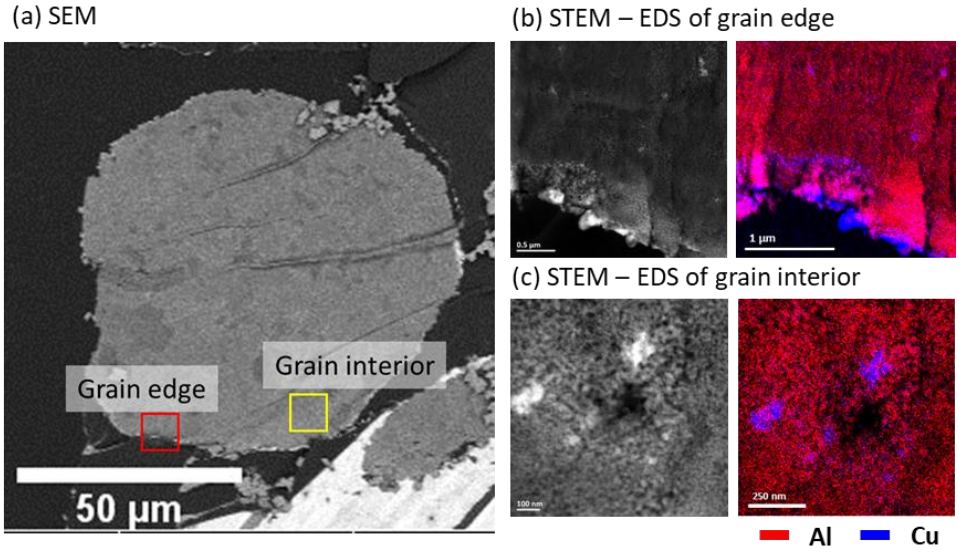

Figure S.17: a) SEM image and b) STEM-EDS with Cu-Al distribution at the grain edge and (c) inside the grain of the CuO/Al_2O_3-700 sample cycled at 700 °C, after 50 cycles.

SI.5.6. 700 – 200 cycles

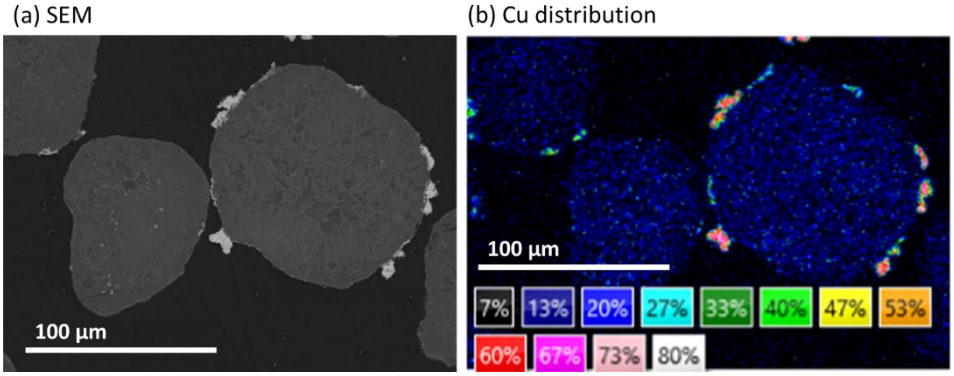

Figure S.18: a) SEM image and b) EDS Cu-concentration map of the sample cycled at 700 °C, after 200 cycles.

References

[1] Belkhou, R.; Stanescu, S.; Swaraj, S.; Besson, A.; Ledoux, M.; Hajlaoui, M.; Dalle, D. HERMES: A Soft X-Ray Beamline Dedicated to X-Ray Microscopy. *J Synchrotron Rad* 2015, *22* (4), 968–979. https://doi.org/10.1107/S1600577515007778.

[2] AXis2000 Is an Application Written in Interactive Data Language. It Is Available Free for Noncommercial Applications at Http://Unicorn.Mcmaster.ca/AXis2000.Html.

[3] de Groot, F. M. F.; de Smit, E.; van Schooneveld, M. M.; Aramburo, L. R.; Weckhuysen, B. M. In-Situ Scanning Transmission X-Ray Microscopy of Catalytic Solids and Related Nanomaterials. *ChemPhysChem* 2010, *11* (5), 951–962. https://doi.org/10.1002/cphc.200901023.

[4] Https://Henke.Lbl.Gov/Optical_constants/Atten2.Html.

[5] Cassinelli, W. H.; Martins, L.; Passos, A. R.; Pulcinelli, S. H.; Santilli, C. V.; Rochet, A.; Briois, V. Multivariate Curve Resolution Analysis Applied to Time-Resolved Synchrotron X-Ray Absorption Spectroscopy Monitoring of the Activation of Copper Alumina Catalyst. *Catalysis Today* 2014, *229*, 114–122. https://doi.org/10.1016/j.cattod.2013.10.077.

[6} Tangcharoen, T.; Klysubun, W.; Kongmark, C. Synchrotron X-Ray Absorption Spectroscopy and Cation Distribution Studies of NiAl2O4, CuAl2O4, and ZnAl2O4 Nanoparticles Synthesized by Sol-Gel Auto Combustion Method. *Journal of Molecular Structure* 2019, *1182*, 219–229. https://doi.org/10.1016/j.molstruc.2019.01.049.

[7] Daichakomphu, N.; Sakulkalavek, A.; Sakdanuphab, R. Effects of Iron Doping on the Oxidation/Reduction Properties of Delafossite CuAlO2 Synthesized via a Solid-State Reaction. *J Mater Sci: Mater Electron* 2020, *31* (12), 9481–9485. https://doi.org/10.1007/s10854-020-03488-3.

[8] Shimizu, K.; Maeshima, H.; Yoshida, H.; Satsuma, A.; Hattori, T. Spectroscopic Characterisation of Cu–Al2O3 Catalysts for Selective Catalytic Reduction of NO with Propene. *Phys. Chem. Chem. Phys.* 2000, *2* (10), 2435–2439. https://doi.org/10.1039/b000943l.

[9] Bolt, P. H.; Habraken, F. H. P. M.; Geus, J. W. Formation of Nickel, Cobalt, Copper, and Iron Aluminates Fromα- Andγ-Alumina-Supported Oxides: A Comparative Study. *Journal of Solid State Chemistry* 1998, *135* (1), 59–69. https://doi.org/10.1006/jssc.1997.7590.